

Graph automorphism group of the dissociation microequilibrium of polyprotic acids

Nicolás Salas, Justin López, and Carlos A. Arango*

Department of Pharmaceutical and Chemical Sciences, Universidad Icesi, Cali, Colombia

E-mail: caarango@icesi.edu.co

Abstract

The dissociation micro-states (DMS) of an N -protic acid are described using set theory notation. This facilitates the mathematical description of the dissociation micro-equilibrium (DME). In particular, the DME constants are easily obtained in terms of the dissociation equilibrium constants and the molar fractions of the DMSs. Representing of the DMEs in terms of graph theory allows to identify permutations between DMSs that preserve the vertex-edge connectivity of the graph. These permutations, along with their composition, allow us to identify the direct product of the cyclic group C_2 , and the symmetric group S_N , $C_2 \times S_N$, as the graph automorphism group of the micro-dissociation of N -protic acids.

Introduction

Chemical applications of Graph Theory have origin in the earlier works on the enumeration of chemical isomers [1–7] and the depiction of molecules [6, 8]. To date, there are numerous chemical applications of graph theory in research fields such as biochemistry, chemical kinetics, catalysis, quantum chemistry, NMR spectroscopy, chemoinformatics, and new drug discovery, among others [9–13]. In chemoinformatics, graph theory has been instrumental

in finding similarities between molecules to discover new drugs [14, 15]. Applications of graph theory to chemical reaction networks have allowed the description and representation of complex reaction mechanisms using topological and complexity indices [16–22]. Reaction networks and graph theory have been used to study the dissociation of weak acids and bases. For example, the method of exponential polytopes has been employed to obtain approximate formulas for the pH of monoprotic weak acids [17]. Graph kernels have been utilized to estimate acid/base dissociation constants in molecules of biopharmaceutical interest [23]. Graph convolutional neural networks have been used for predicting the pK_a values and protonation state distribution of molecules of pharmaceutical interest [24]. In homogeneous catalysis graph-theoretical methodology has been proposed for the exploration of the chemical reaction space of multicomponent mixtures [13]. In quantum chemistry weighted-graph-theoretical approaches are used to compute contributions from many-body approximations in post-Hartree-Fock molecular dynamics [25].

In biochemistry, graph theory methods have been employed to analyze the covalent and non-covalent bond networks in proteins, allowing for the identification of flexible and rigid regions in these biomolecules [26]. Additionally, in biochemistry, graph convolutional networks have been used for automated function prediction of proteins from the protein structure [27]. Dynamical graph analysis of the hydrogen bond network has allowed to study structural changes in membrane proteins, and the identification of protein groups relevant for proton transfer activity [28].

Algebraic graph theory applies algebraic methods to graphs [29]. The connection between graphs and group theory is one of the main branches of algebraic graph theory [30]. The permutations of the vertices of a graph that maintain the edge-vertex connectivity endowed with the composition operation define the automorphism group of the graph. In chemistry obtaining the automorphism group of a an associated graph is important in spectroscopy, quantum chemistry, structural elucidation and prediction of NMR spectrum of molecules, and in the characterization of molecular complexity, among other applications [31–35].

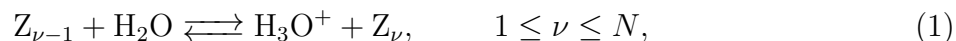
A polyprotic Brønsted-Lowry acid is a substance capable of donating more than one proton [36, 37]. These protons are released one by one in the consecutive (macroscopic) model, from the most acidic to the least acidic. The concentration of the chemical species involved in the consecutive dissociation model are obtained from the macroscopic equilibrium constants, the auto-ionization of water, and the balances of mass and charge of the acid dissolution [38–41]. In the non-consecutive (microscopic) dissociation model, the N protons are released independently. The concentrations of the chemical species involved in the non-consecutive dissociation are obtained from the micro-equilibrium constants, the auto-ionization of water, and the balances of charge and mass [42, 43]. Micro-equilibrium constants and concentrations are important in biochemistry and pharmaceutical sciences [44–50]. The relations between microscopic and macroscopic equilibrium constants of polyprotic acids were developed by Hill [51].

This work is organized as follows. Sections and are used to introduce the consecutive and non-consecutive acid dissociation models, respectively, along with the corresponding notation based on sets. Section demonstrate that the use of a notation based on set theory simplifies the complicated expression obtained by Hill in terms of indices, allowing for a general expression to be derived for the micro-equilibrium constants. These are expressed in terms of the equilibrium constants and the molar fractions of the tautomers of the acid's dissociation states. Examples of the diprotic and triprotic acids are provided in section . In section , the use of graph theory to represent the micro-dissociation of polyprotic acids and to obtain their graph automorphism group is explored. The aqueous dissociation of monoprotic, diprotic, and triprotic acids is thoroughly examined, identifying $\text{aut}(G_N) = C_2 \times S_N$ as the automorphism group of the N -protic acid dissociation.

Theory and Methods

Consecutive dissociation of polyprotic acids

The aqueous dissociation equilibrium of a polyprotic weak acid H_NB is given by N consecutive acid dissociations plus the water auto-ionization,



respectively. The equilibria displayed by equations (1) and (2) are effective equilibria since the N protons of H_NB can dissociate separately and not necessarily consecutively [42, 43, 48]. The acid H_NB has $N + 1$ deprotonation states (DS)

$$Z_\nu = H_{N-\nu}B^{\nu-}, \quad \nu = 0, 1, 2, \dots, N, \quad (3)$$

with $Z_0 = H_NB$ as the fully protonated state, and $Z_N = B^{N-}$ as the fully deprotonated state. The activities of the DSs Z_ν are given by $a_\nu(Z_\nu) = \gamma_\nu[Z_\nu]/C^\circ$, with γ_ν as the molar activity coefficient, $[Z_\nu]$ as the molar concentration, and $C^\circ = 1$ M. The activities of the hydronium and hydroxide ions are given by $a(H_3O^+) = \gamma_{H_3O^+}[H_3O^+]/C^\circ$ and $a(OH^-) = \gamma_{OH^-}[OH^-]/C^\circ$, with $[H_3O^+]$ and $[OH^-]$ as the molar concentrations of the hydronium and hydroxide ions.

The equilibrium state of a N -protic acid at analytical concentration C_a is mathematically characterized by $N + 3$ equations: the N equilibrium constants, the water autoionization

constant, and the balances of charge and mass

$$K_\nu = \frac{a(Z_\nu)a(\text{H}_3\text{O}^+)}{a(Z_{\nu-1})}, \quad \nu = 1, 2, \dots, N, \quad (4)$$

$$K_w = a(\text{H}_3\text{O}^+)a(\text{OH}^-), \quad (5)$$

$$[\text{H}_3\text{O}^+] = [\text{OH}^-] + \sum_{\nu=0}^N \nu [Z_\nu], \quad (6)$$

$$C_a = \sum_{\nu=0}^N [Z_\nu], \quad (7)$$

respectively. In the case of diluted solutions, it is valid to use the approximations $a(Z_\nu) \approx [Z_\nu]/C^\circ$, $a(\text{H}_3\text{O}^+) \approx [\text{H}_3\text{O}^+]/C^\circ$, and $a(\text{OH}^-) \approx [\text{OH}^-]/C^\circ$. The use of the biochemical standard state, $C^\ominus = 10^{-7}C^\circ$, to define the dimensionless quantities $z_\nu = [Z_\nu]/C^\ominus$, $x = [\text{H}_3\text{O}^+]/C^\ominus$, and $y = [\text{OH}^-]/C^\ominus$, allows to rewrite equations (4) to (7) as

$$k_\nu = \frac{z_\nu x}{z_{\nu-1}}, \quad \nu = 1, 2, \dots, N, \quad (8)$$

$$1 = xy, \quad (9)$$

$$x = y + \sum_{\nu=0}^N \nu z_\nu, \quad (10)$$

$$c_a = \sum_{\nu=0}^N z_\nu, \quad (11)$$

with $c_a = C_a/C^\ominus$, $k_w = 1$, and $k_\nu = 10^7 K_\nu$.

This N -protic acid has N distinguishable sites, each capable of being either occupied by a proton or left unoccupied. In this context, the dissociation state Z_ν is characterized by having $N - \nu$ occupied sites and ν unoccupied sites. The sites of H_NB are in one-to-one correspondence with the elements of the set $S_N = \{1, 2, \dots, N\}$.

There are two distinct deprotonation schemes: consecutive and non-consecutive. In consecutive or sequential acid dissociation, protons on the occupied sites are released in a specific, predetermined order. Formally, this order is given by an enumeration of S_N ,

$\mathcal{E} = (\nu_1, \nu_2, \dots, \nu_N)$, where

$$\begin{aligned}\nu_1 &\in S_N, \\ \nu_2 &\in S_N - \{\nu_1\}, \\ \nu_3 &\in S_N - \{\nu_1, \nu_2\}, \dots, \\ \nu_n &\in S_N - \{\nu_1, \nu_2, \dots, \nu_{n-1}\}, \dots, \\ \nu_N &\in S_N - \{\nu_1, \nu_2, \dots, \nu_{N-1}\}.\end{aligned}$$

In the consecutive dissociation there is a one-to-one mapping between the states Z_μ and the sets $S_N - \{\nu_1, \nu_2, \dots, \nu_\mu\}$, with Z_0 mapped to S_N , Z_1 mapped to $S_N - \{\nu_1\}$, ..., Z_{N-1} mapped to $S_N - \{\nu_1, \nu_2, \dots, \nu_{N-1}\}$, and Z_N mapped to \emptyset .

Nonconsecutive dissociation of polyprotic acids

On the other hand, in non-consecutive acid dissociation, the protons can separate independently instead of consecutively. Dissociation micro-states (DMS) are necessary to describe the non-consecutive acid dissociation. In the non-consecutive dissociation, the dissociation state Z_ν has $\binom{N}{\nu} = \frac{N!}{(N-\nu)!\nu!}$ possible dissociation micro-states. these DMSs are given by the subsets of S_N with $N - \nu$ elements. The set of micro-states of Z_ν is given by

$$M_\nu = \{T \in \mathcal{P}(S_N) : |T| = N - \nu\}, \quad (12)$$

with $\mathcal{P}(S_N)$ as the power set of S_N , defined as:

$$\mathcal{P}(S_N) = \{T : T \subseteq S_N\}. \quad (13)$$

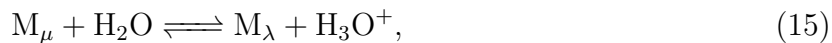
In simpler terms, M_ν represents the collection of all subsets of S_N with $N - \nu$ elements, each corresponding to a unique DMS of Z_ν . The DMSs of Z_ν are given by M_μ with

$\mu \in M_\nu$. For example, the DS Z_1 of a 3-protic acid has $\binom{3}{1} = 3$ DMSs M_μ , with $\mu \in M_1 = \{\{1, 2\}, \{1, 3\}, \{2, 3\}\}$. The fully protonated and fully deprotonated state Z_0 and Z_N respectively, have only one DMS each M_{S_N} and M_\emptyset , respectively. An N -protic acid has a total of 2^N DMSs.

The molar concentration of the deprotonation state Z_ν , $[Z_\nu]$, is related to the molar concentrations of its deprotonation microstates, $[M_\mu]$, by

$$[Z_\nu] = \sum_{\mu \in M_\nu} [M_\mu], \quad \nu \in S_N. \quad (14)$$

The micro-equilibria of deprotonation and protonation (DME and PME, respectively) between the DMSs M_μ and M_λ are possible when the absolute difference between the sets μ and λ is 1, and either $\mu \subsetneq \lambda$ or $\lambda \subsetneq \mu$. These micro-equilibria are given by the chemical equations



and the micro-equilibrium constants

$$K_{\mu\lambda} = \frac{a(M_\lambda)a(\text{H}_3\text{O}^+)}{a(M_\mu)}, \quad (17)$$

$$K_{\lambda\mu} = \frac{a(M_\mu)a(\text{OH}^-)}{a(M_\lambda)}. \quad (18)$$

The activities of M_μ , M_λ , H_3O^+ and OH^- , are given by

$$\begin{aligned} a(M_\mu) &= \gamma_\mu [M_\mu]/C^\circ, & a(M_\lambda) &= \gamma_\lambda [M_\lambda]/C^\circ, \\ a(\text{H}_3\text{O}^+) &= \gamma_{\text{H}_3\text{O}^+} [\text{H}_3\text{O}^+]/C^\circ, \text{ and} & a(\text{OH}^-) &= \gamma_{\text{OH}^-} [\text{OH}^-]/C^\circ, \end{aligned}$$

respectively, with $C^\circ = 1 \text{ M}$ as the standard state, and γ_μ , γ_λ , $\gamma_{\text{H}_3\text{O}^+}$, and γ_{OH^-} , as the

activity coefficients. The addition of the chemical equations (15) and (16) gives the water autoionization equilibrium



which has equilibrium constant

$$\begin{aligned} K_w &= K_{\mu\lambda}K_{\lambda\mu} \\ &= a(\text{H}_3\text{O}^+)a(\text{OH}^-). \end{aligned} \quad (20)$$

Although the number of micro-equilibrium constants between the DMSs of $Z_{\nu-1}$ and Z_ν is given by $2\binom{N}{\nu-1}\binom{N}{\nu}$, only $2\binom{N}{\nu}(N-\nu)$ are chemically related. The set of chemically related DME constants is given by

$$K = \{K_{\mu\lambda} : \mu \subsetneq \lambda \text{ or } \lambda \subsetneq \mu, \text{abs}(|\mu| - |\lambda|) = 1\}. \quad (21)$$

The total number of DMEs and PME for a N -protic acid is $2^N N$. The 3-protic acid can be used as an example. The DMS of Z_1 and Z_2 are given by M_μ and M_λ respectively, with $\mu \in M_1$ and $\lambda \in M_2$ as elements of the sets $M_1 = \{\{2, 3\}, \{1, 3\}, \{1, 2\}\}$ and $M_2 = \{\{1\}, \{2\}, \{3\}\}$, respectively. Since $\{3\} \not\subset \{1, 2\}$, or $\{1, 2\} \not\subset \{3\}$, there are not DME between the DMSs $\{1, 2\}$ of Z_1 and $\{3\}$ of Z_2 . On the other hand, since $\{1\} \subsetneq \{1, 2\}$, and $\text{abs}(|\{1, 2\}| - |\{1\}|) = 1$, there are DME and PME between $\{1, 2\}$ and $\{1\}$. The total number of DME and PME for the 3-protic acid is $3 \times 2^3 = 24$.

In the case of aqueous dilute solutions all the activity coefficients are approximately one, and it is justified to use the approximations $a(M_\mu) \approx [M_\mu]/C^\circ$, $a_{\text{OH}^-} \approx [\text{OH}^-]/C^\circ$, and $a_{\text{H}_3\text{O}^+} \approx [\text{H}_3\text{O}^+]/C^\circ$. The use of the biochemical standard state $C^\ominus = 10^{-7}C^\circ$, allows to

write the micro-equilibrium constants (17), (18), and (20) as

$$k_{\mu\lambda} = \frac{xm_\lambda}{m_\mu}, \quad (22)$$

$$k_{\lambda\mu} = \frac{ym_\mu}{m_\lambda}, \quad (23)$$

$$1 = xy, \quad (24)$$

respectively. It can be shown that $k_{\mu\lambda} = 10^7 K_{\mu\lambda}$ and $k_{\lambda\mu} = 10^7 K_{\lambda\mu}$.

Relation between dissociation equilibria and micro-equilibria

There is a simple relation between the deprotonation equilibrium constants k_ν , with $\nu \in S_N$, and the deprotonation micro-equilibrium constants, $k_{\mu\lambda}$, with $\mu \in M_{\nu-1}$, and $\lambda \in M_\nu$. The deprotonation equilibrium constant k_ν ,

$$k_\nu = \frac{xz_\nu}{z_{\nu-1}}, \quad \nu \in S_N, \quad (25)$$

can be written in terms of the deprotonation micro-states

$$k_\nu = \frac{x \sum_{m_\lambda \in M_\nu} m_\lambda}{\sum_{m_\mu \in M_{\nu-1}} m_\mu}. \quad (26)$$

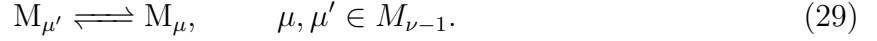
The reciprocal of k_ν is given by

$$\begin{aligned} \frac{1}{k_\nu} &= \sum_{\mu \in M_{\nu-1}} \frac{m_\mu}{x \sum_{\lambda \in M_\nu} m_\lambda} \\ &= \sum_{\mu \in M_{\nu-1}} \left(\sum_{\lambda \in M_\nu} \frac{xm_\lambda}{m_\mu} \right)^{-1} \\ &= \sum_{\mu \in M_{\nu-1}} \left(\sum_{\lambda \in M_\nu} k_{\mu\lambda} \right)^{-1}. \end{aligned} \quad (27)$$

A simpler relation between the equilibrium constants k_ν and the micro-equilibrium constants can be obtained by dividing numerator and denominator of the right hand side of equation (26) by $m_{\mu'}$ with $\mu' \in M_{\nu-1}$,

$$\begin{aligned} k_\nu &= \frac{x \sum_{\lambda \in M_\nu} m_\lambda / m_{\mu'}}{\sum_{\mu \in M_{\nu-1}} m_\mu / m_{\mu'}} \\ &= \frac{\sum_{\lambda \in M_\nu} k_{\mu'\lambda}}{\sum_{\mu \in M_{\nu-1}} \tau_{\mu'\mu}}, \end{aligned} \quad (28)$$

with $\tau_{\mu'\mu} = m_\mu / m_{\mu'}$ as the equilibrium constant for the tautomerization (isomerization) between the protonation micro-states M_μ and $M_{\mu'}$ of $Z_{\nu-1}$,



Equation (28) can be written in terms of the molar fractions $x_\mu = m_\mu / z_\nu$ for $\mu \in M_\nu$,

$$k_\nu = x_\mu \sum_{\lambda \in M_\nu} k_{\mu\lambda}, \quad \mu \in M_{\nu-1}. \quad (30)$$

It is easy to verify that the micro-equilibrium and tautomerization constants are related by:

$$k_{\mu'\lambda} = \tau_{\mu'\mu} k_{\mu\lambda}, \quad (31)$$

$$k_{\mu\lambda'} = k_{\mu\lambda} \tau_{\lambda\lambda'}. \quad (32)$$

An expression for the micro-equilibrium constants, in terms of the equilibrium constants and the microscopic molar fractions, can be obtained from the general definition of the micro-dissociation constants, $k_{\mu\lambda} = x m_\lambda / m_\mu$, for $\mu \in M_{\nu-1}$ and $\lambda \in M_\nu$. Multiplying the numerator of this expression by the unity $1 = z_\nu / z_\nu$, and the denominator by the unity $1 = z_{\nu-1} / z_{\nu-1}$, gives after rearranging terms

$$k_{\mu\lambda} = \frac{x_\lambda}{x_\mu} k_\nu, \quad \mu \in M_{\nu-1}, \lambda \in M_\nu. \quad (33)$$

This expression has been used previously, for the diprotic acid, in order to get the micro-equilibrium constants from the equilibrium constants and measurements of ^{13}C NMR [52].

Graph-Theory description of polyprotic acids micro-dissociation

In graph theory, a graph $G = (V, E)$ is a structure built from a set of vertices V , and a set of edges, E . The elements of E are the relations between pairs of vertices. Directed and undirected edges indicate one-way and two-way relationships between two vertices, respectively. Directed edges are written in parenthesis meanwhile undirected edges are written in curly brackets.

The dissociation of a N -protic acid can be represented by a graph $G_N = (V_N, E_N)$, with $V_N = \{M_\mu : \mu \in \mathcal{P}(S_N)\}$, and E_N given by the set $E_N = P_k(S_N) \cup P_\tau(S_N)$ with

$$P_k(S_N) = \{\{M_\mu, M_\lambda\}, \mu \in \mathcal{P}(S_N), \lambda \in \mathcal{P}(S_N) : \mu \subsetneq \lambda \text{ or } \lambda \subsetneq \mu, \text{abs}(|\mu| - |\lambda|) = 1\}, \quad (34)$$

$$P_\tau(S_N) = \{\{M_\mu, M_\lambda\}, \mu \in \mathcal{P}(S_N), \lambda \in \mathcal{P}(S_N) : |\mu| = |\lambda| = |\mu \cap \lambda| + 1\}, \quad (35)$$

where P_k is the set of pairs of DMSs related by micro-equilibrium constants, and P_τ is the set of pairs of DMSs related by tautomerization constants.

The microequilibrium and tautomerization constants of acid dissociation always occur in pairs. For every $k_{\mu\lambda}$ and $\tau_{\mu\mu'}$, there exist $k_{\lambda\mu}$ and $\tau_{\mu'\mu}$, respectively. This pairing of constants allows undirected edges to represent pairs of equilibrium and tautomerization constants in the graph G_N .

A graph automorphism of G_N is a permutation, denoted σ , of the set of vertices, V_N , that maintains the edge-vertex connectivity of G_N . Because the compositions of two permutations is also a permutation, the composition of two graph automorphisms must likewise be a graph automorphism. The set of automorphism of G_N , equipped with the composition of automorphisms, constitutes a group known as the graph automorphism group of G_N , denoted $\text{aut}(G_N)$.

Relation between equilibrium and micro-equilibrium constants for diprotic and triprotic acids

In the case of a diprotic acid the concentration vectors of dissociation and micro-dissociation states are $\mathbf{z}^\top = \{z_0, z_1, z_2\}$, and

$$\begin{aligned} \mathbf{m}^\top &= \{m_{\{1,2\}}, m_{\{2\}}, m_{\{1\}}, m_\emptyset\} \\ &= \{m_{12}, m_2, m_1, m_0\}, \end{aligned} \tag{36}$$

respectively. The second line of the equation defining \mathbf{m} was obtained by applying the assignation rules $\emptyset \rightarrow 0$, $\{1\} \rightarrow 1$, $\{2\} \rightarrow 2$, and $\{1,2\} \rightarrow 12$. In these terms, the vectors of dissociation and micro-dissociation constants are given by $\mathbf{k}^\top = \{k_1, k_2\}$, and $\tilde{\mathbf{k}}^\top = \{k_{12,1}, k_{12,2}, k_{1,0}, k_{2,0}\}$.

The use of equations (28), (31) and (32) produces the linear system of equations

$$k_1 = k_{12,1} + k_{12,2}, \tag{37}$$

$$k_2(1 + \tau) = k_{12,1}, \tag{38}$$

$$k_2(1 + \tau) = \tau k_{12,2}, \tag{39}$$

$$0 = \tau k_{10} - k_{20} \tag{40}$$

$$0 = k_{12,1} - \tau k_{12,2}, \tag{41}$$

where $\tau = \tau_{12}$. It is easy to verify that the combined use of these equations gives the dissociation constants, \mathbf{k} , in terms of the micro-dissociation constants, $\tilde{\mathbf{k}}$. The first dissociation constant is already given by equation (37), $k_1 = k_{12,1} + k_{12,2}$; The second dissociation constant is obtained by substitution of τ from equation (41) in equation (38) to obtain

$$k_2 = \frac{k_{12,1}k_{12,2}}{k_{12,1} + k_{12,2}}. \tag{42}$$

The micro-dissociation constants, $\tilde{\mathbf{k}}$, in terms of \mathbf{k} and τ are given by

$$\begin{aligned}
k_{12,1} &= x_1 k_1, \\
k_{12,2} &= x_2 k_1, \\
k_{1,0} &= x_1^{-1} k_2, \\
k_{2,0} &= x_2^{-1} k_2,
\end{aligned} \tag{43}$$

with $x_1 = m_1/z_1$ and $x_2 = m_2/z_1$.

The dissociation of the triprotic acid is a more interesting example. The concentration vector of dissociation states is $\mathbf{z} = \{z_0, z_1, z_2\}$. The concentration vector of the micro-dissociation states is

$$\mathbf{m}^\top = \{m_{S_3}, m_{23}, m_{13}, m_{12}, m_3, m_2, m_1, m_0\}. \tag{44}$$

The vectors of dissociation constants \mathbf{k} , and micro-dissociation constants $\tilde{\mathbf{k}}$, are given by $\mathbf{k}^\top = \{k_1, k_2, k_3\}$ and

$$\begin{aligned}
\tilde{\mathbf{k}}^\top &= \{k_{S_3,23}, k_{S_3,13}, k_{S_3,12}, k_{23,2}, k_{23,3}, k_{13,1}, k_{13,3}, k_{12,1}, k_{12,2}, \\
& k_{30}, k_{20}, k_{10}\}.
\end{aligned} \tag{45}$$

There are three possible tautomerizations between the dissociation micro-states $M_2 = \{1, 2, 3\}$.

The use of equations (31) and (32) gives

$$\tau_{12} = \frac{k_{20}}{k_{10}} = \frac{k_{12,1}}{k_{12,2}}, \tag{46}$$

$$\tau_{13} = \frac{k_{30}}{k_{10}} = \frac{k_{13,1}}{k_{13,3}}, \tag{47}$$

$$\tau_{23} = \frac{k_{30}}{k_{20}} = \frac{k_{23,2}}{k_{23,3}}. \tag{48}$$

In the same way, there are three tautomerizations between the dissociation micro-states

$$M_1 = \{12, 13, 23\}$$

$$\tau_{12,13} = \frac{k_{13,1}}{k_{12,1}} = \frac{k_{S_3,12}}{k_{S_3,13}}, \quad (49)$$

$$\tau_{12,23} = \frac{k_{23,2}}{k_{12,2}} = \frac{k_{S_3,12}}{k_{S_3,23}}, \quad (50)$$

$$\tau_{13,23} = \frac{k_{23,3}}{k_{13,3}} = \frac{k_{S_3,13}}{k_{S_3,23}}. \quad (51)$$

The tautomerization constants are related between them by

$$\tau_{13} = \tau_{12}\tau_{23}, \quad (52)$$

$$\tau_{12,23} = \tau_{12,13}\tau_{13,23}. \quad (53)$$

The use of equation (28) with $\nu = 1$ gives first dissociation constant of the triprotic acid $k_1 = k_{S_3,1} + k_{S_3,2} + k_{S_3,3}$. Equation (28) with $\nu = 2$ gives three equations for k_2 , which are all equivalent to

$$(1 + \tau_{12} + \tau_{13})k_2 = k_{12,1} + k_{13,1} + \tau_{12}k_{23,2}. \quad (54)$$

The use of the tautomerizations (46)-(48), in terms of the dissociation micro-states of Z_1 , gives

$$k_2 = \frac{k_{13,3} (k_{12,1}k_{12,2} + k_{13,1}k_{12,2} + k_{12,1}k_{23,2})}{k_{13,1}k_{12,2} + k_{12,1}k_{13,3} + k_{12,2}k_{13,3}}. \quad (55)$$

This is only one of three possible (equivalent) equations for k_2 . The third dissociation constant of the triprotic acid gives also three equations equivalent to

$$(1 + \tau_{12,13} + \tau_{12,23})k_3 = k_{S_3,12}. \quad (56)$$

This equation gives $k_{S_3,12} = x_{12}^{-1}k_3$. The use of the tautomerizations (49)-(51), in terms of

the dissociation micro-states of S_2 , in equation (56) gives

$$k_3 = \frac{k_{S_3,12}k_{S_3,13}k_{S_3,23}}{k_{S_3,12}k_{S_3,13} + k_{S_3,12}k_{S_3,23} + k_{S_3,13}k_{S_3,23}}. \quad (57)$$

Again, this is only one of three possible (equivalent) equations for k_3 .

The use of the tautomerizations (47) and(48) in $k_1 = k_{S_3,1} + k_{s_3,2} + k_{S_3,3}$ gives

$$k_{S_3,1} = \frac{k_1}{1 + \tau_{12} + \tau_{13}} = x_1 k_1. \quad (58)$$

The constants $k_{S_3,2}$ and $k_{S_3,3}$ are obtained from equations (46) and (47)

$$k_{S_3,2} = \tau_{12}k_{S_3,1} = x_2 k_1, \quad (59)$$

$$k_{S_3,3} = \tau_{13}k_{S_3,1} = x_3 k_1. \quad (60)$$

The constant $k_{12,1}$ is obtained from equation (54) and the tautomerizations. The substitutions $k_{13,1} = \tau_{12,13}k_{12,1}$ and $\tau_{12}k_{23,2} = \tau_{12,23}k_{12,1}$ in (54) gives

$$k_{12,1} = \frac{1 + \tau_{12} + \tau_{13}}{1 + \tau_{12,13} + \tau_{12,23}} k_2 = \frac{x_{12}}{x_1} k_2. \quad (61)$$

The other constants of $\tilde{\mathbf{k}}$ are obtained from $k_{12,1}$ and the tautomerizations

$$k_{13,1} = \tau_{12,13}k_{12,1} = \frac{x_{13}}{x_1} k_2, \quad (62)$$

$$k_{12,2} = \frac{k_{12,1}}{\tau_{12}} = \frac{x_{12}}{x_2} k_2, \quad (63)$$

$$k_{23,2} = \frac{\tau_{12,23}}{\tau_{12}} k_{12,1} = \frac{x_{23}}{x_2} k_2, \quad (64)$$

$$k_{13,3} = \frac{\tau_{12,13}}{\tau_{13}} k_{12,1} = \frac{x_{13}}{x_3} k_2, \quad (65)$$

$$k_{23,3} = \frac{\tau_{12,23}}{\tau_{13}} k_{12,1} = \frac{x_{23}}{x_3} k_2. \quad (66)$$

Finally the constants $k_{S_3,\mu}$, $\mu \in M_2$, are given by equation (56) and

$$k_{S_3,13} = \frac{1}{\tau_{12,13}} k_{S_3,12} = x_{13}^{-1} k_3, \quad (67)$$

$$k_{S_3,23} = \frac{1}{\tau_{12,23}} k_{S_3,12} = x_{23}^{-1} k_3. \quad (68)$$

Graph automorphism groups of the dissociation of polyprotic acids

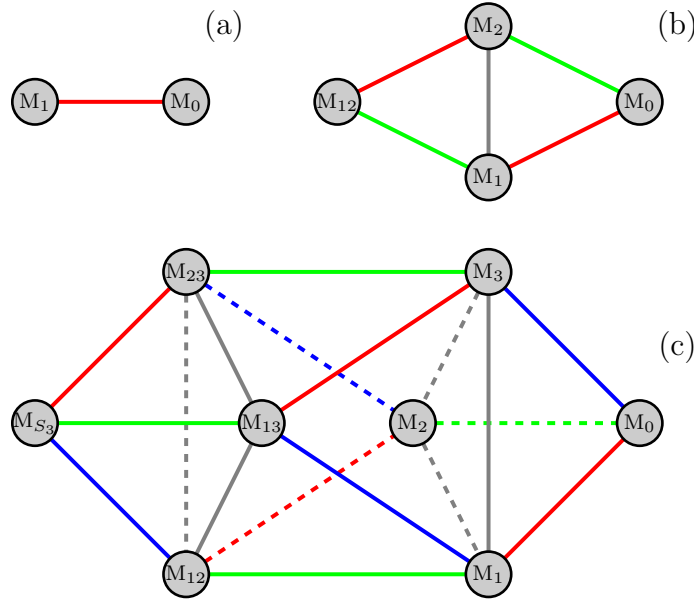


Figure 1: Dissociation graphs of some polyprotic acids. (a) Monoprotic acid; (b) Diprotic acid; (c) Triprotic acid. Red, green and blue edges represent the deprotonation/protonation of protons (1), (2), and (3), respectively, gray edges represent tautomerizations. Dashed edges are used to facilitate the visualization of G_3 .

In the case of a monoprotic acid, the sets V_1 and E_1 are $V_1 = \{M_1, M_0\}$ and $E_1 = \{\{M_1, M_0\}\}$. The graph $G_1 = (V_1, E_1)$ is depicted in figure 1(a). This graph is known as the complete graph of order two, denoted as K_2 , where all vertices are connected by edges. The acid-base permutation

$$\sigma_{10} = (M_1 M_0)(H_3O^+ OH^-), \quad (69)$$

exchanges M_1 with M_0 , and H_3O^+ with OH^- . In terms of concentrations, σ_{10} exchanges m_1 with m_0 , and x with y . The effect of σ_{10} on the micro-equilibrium constants is given by

$\sigma_{10}(k_{10}) = k_{01}$ and $\sigma_{10}(k_{01}) = k_{10}$. The graph G_1 is shown to be preserved under the action of σ_{10} in figure 2. This means σ_{10} maps G_1 onto itself without losing edge connectivity, making σ_{10} a graph automorphism of G_1 . The identity permutation $e = (M_1)(M_0)(H_3O^+)(OH^-)$ is also a graph automorphism of G_1 . Under the operation of composition, the graph automorphisms e and σ_{10} generate the graph automorphism group of G_1 , denoted as $\text{aut}(G_1) = \langle \sigma_{10} \rangle$. The permutation σ_{10} is an involution, meaning $\sigma_{10} = \sigma_{10}^{-1}$, hence $\sigma_{10}^2 = e$ establishes a condition on the generators of the group. The group presentation is given as

$$\text{aut}(G_1) = \langle \sigma_{10} | \sigma_{10}^2 = e \rangle, \quad (70)$$

which specifies that the cyclic group of order two, C_2 , represents the monoprotic acid dissociation.

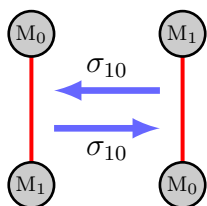


Figure 2: Effect of the permutations σ_{10} on the graph G_1 .

The dissociation of a diprotic acid is represented by the graph $G_2 = (V_2, E_2)$ with

$$V_2 = \{M_{12}, M_2, M_1, M_0\}, \quad (71)$$

$$E_2 = \{\{M_{12}, M_2\}, \{M_{12}, M_1\}, \{M_1, M_2\}, \{M_2, M_0\}, \{M_1, M_0\}\}. \quad (72)$$

The graph $G_2 = (V_2, E_2)$ of the diprotic acid micro-dissociations is depicted in figure 1(b). In this graph, red and green edges represent two types of micro-dissociations. The red edges correspond to the dissociations of protons occupying site 1, while the green edges correspond to protons at site 2. The gray edge represents the tautomerization between the DMSs M_1 and M_2 . The graph G_2 of the diprotic acid micro-dissociations is a complete tripartite graph, $G_2 = K_{1,1,2}$, also known as the diamond graph. The acid-base permutation $\sigma_{12,0}$, and the

tautomerization permutation σ_{21} are defined as:

$$\sigma_{12,0} = (M_{12}M_0)(H_3O^+OH^-), \quad (73)$$

$$\sigma_{21} = (M_2M_1)(H_3O^+)(OH^-). \quad (74)$$

These permutations preserve the edge-vertex connectivity of G_2 , as shown in figure 3. Under the composition operation, the graph automorphisms $\sigma_{12,0}$, σ_{21} , and the identity e , form the graph automorphism group of G_2 , denoted $\text{aut}(G_2) = \langle \sigma_{12,0}, \sigma_{21} \rangle$. Since the permutations $\sigma_{12,0}$ and σ_{21} are involutions (self-inverses), the graph automorphism group of G_2 is given by

$$\text{aut}(G_2) = \langle \sigma_{12,0}, \sigma_{21} \mid \sigma_{12,0}^2 = \sigma_{21}^2 = (\sigma_{12,0}\sigma_{21})^2 = e \rangle. \quad (75)$$

This is known as Klein's 4-group, or $C_2 \times C_2$. In figure 3, it is evident that the product $\rho = \sigma_{12,0}\sigma_{21}$ results in a counterclockwise rotation of G_2 by π radians. Since C_2 and S_2 are isomorphic ($C_2 \simeq S_2$), the automorphism group of the graph representing the diprotic acid is also expressed as $\text{aut}(G_2) = C_2 \times S_2$.

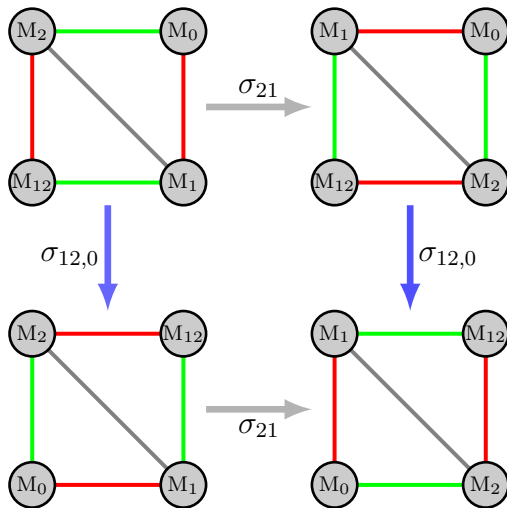


Figure 3: Effect of the permutations $\sigma_{12,0}$ and σ_{21} on the graph G_2 .

The triprotic acid dissociation is characterized by the sets V_3 and E_3 as follows:

$$V_3 = \{M_\mu : \mu \in \mathcal{P}(S_3)\}, \quad (76)$$

$$E_3 = P_k(S_3) \cup P_\tau(S_3), \quad (77)$$

respectively. The graph $G_3 = (V_3, E_3)$ is shown in figure 1(c). This graph displays three types of edges representing deprotonations: proton 1 in red, proton 2 in green, and proton 3 in blue. Tautomerizations are represented by gray edges. There are three permutations that serve as generators of the graph automorphism group of G_3 :

$$\begin{aligned} \sigma_d &= \sigma_{12,23}\sigma_{1,2} \\ &= (M_{12}, M_{23})(M_1, M_2), \end{aligned} \quad (78)$$

$$\begin{aligned} \sigma'_d &= \sigma_{12,13}\sigma_{2,3} \\ &= (M_{12}, M_{13})(M_2, M_3), \end{aligned} \quad (79)$$

$$\begin{aligned} C_2 &= \sigma_{S_3,0}\sigma_{12,1}\sigma_{13,2}\sigma_{23,3} \\ &= (M_{S_3}, M_0)(M_{12}, M_{13})(M_{13}, M_2)(M_{23}, M_3)(H_3O^+OH^-), \end{aligned} \quad (80)$$

The presentation of this group is given by

$$\text{aut}(G_3) = \langle \sigma_d, \sigma'_d, C_2 \mid \sigma_v^2 = (\sigma'_v)^2 = C_2^2 = e \rangle. \quad (81)$$

The effect of these permutations on G_3 is depicted in Figure 4. The permutations (78)-(80) can be interpreted as symmetry operations:

- The tautomerization σ_d acts as a reflection on the plane containing M_{S_3} , M_{12} , M_3 , and M_0 .
- The tautomerization σ'_d is a reflection on the plane containing M_{S_3} , M_{23} , M_1 , and M_0 .
- The acid-base rotation C_2 is a rotation about the axis that goes from the center of the

graph through the midpoint between the DMSs M_{23} and M_3 .

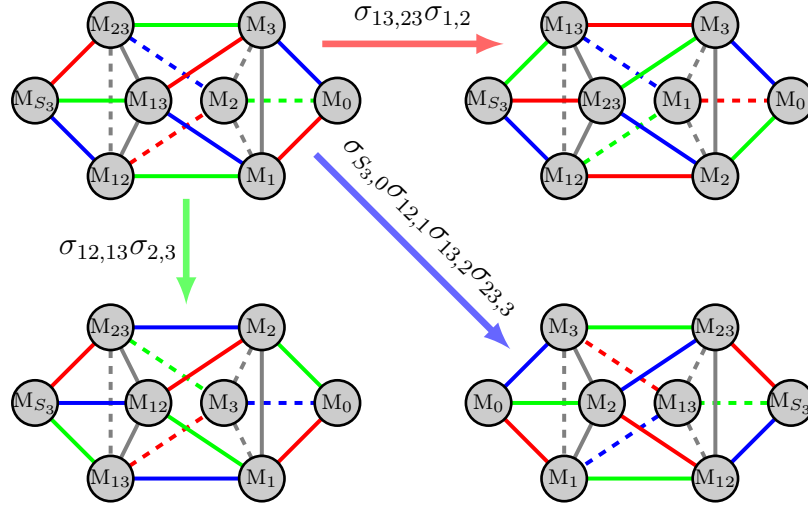


Figure 4: Effect of the permutations $\sigma_{13,23}\sigma_{1,2}$, $\sigma_{12,13}\sigma_{2,3}$, and $\sigma_{S_3,0}\sigma_{12,1}\sigma_{13,2}\sigma_{23,3}$, on the graph G_3 .

Other graph automorphisms of G_3 are

$$\sigma_d'' = (M_{12}, M_{23})(M_1, M_3), \quad (82)$$

$$C_3 = (M_{12}, M_{13}, M_{23})(M_1, M_3, M_2), \quad (83)$$

$$C_3^2 = (M_{12}, M_{23}, M_{13})(M_1, M_2, M_3), \quad (84)$$

$$C_2' = (M_0, M_{S_3})(M_{12}, M_2)(M_{13}, M_3)(M_{23}, M_1)(H_3O^+OH^-), \quad (85)$$

$$C_2'' = (M_0, M_{S_3})(M_{12}, M_3)(M_{13}, M_1)(M_{23}, M_2)(H_3O^+OH^-), \quad (86)$$

$$i = (M_0, M_{S_3})(M_{12}, M_3)(M_{13}, M_2)(M_{23}, M_1)(H_3O^+OH^-), \quad (87)$$

$$S_6 = (M_0, M_{S_3})(M_{12}, M_1, M_{13}, M_3, M_{23}, M_2)(H_3O^+OH^-), \quad (88)$$

$$S_6' = (M_0, M_{S_3})(M_{12}, M_2, M_{23}, M_3, M_{13}, M_1)(H_3O^+OH^-). \quad (89)$$

The graph automorphisms (82)-(89) can be obtained by composition of the generators σ_d ,

σ'_d , and C_2 . A simple inspection gives

$$C_3 = \sigma_d \sigma'_d, \quad (90)$$

$$C_3^2 = \sigma'_d \sigma_d, \quad (91)$$

$$\sigma''_d = C_3 \sigma_d = C_3^2 \sigma'_d, \quad (92)$$

$$S_6 = C_2 \sigma'_d = C_2' \sigma_d, \quad (93)$$

$$S_6' = C_2 \sigma_d, \quad (94)$$

$$C_2'' = i \sigma_d = S_6' \sigma'_d, \quad (95)$$

$$i = C_2' \sigma'_d. \quad (96)$$

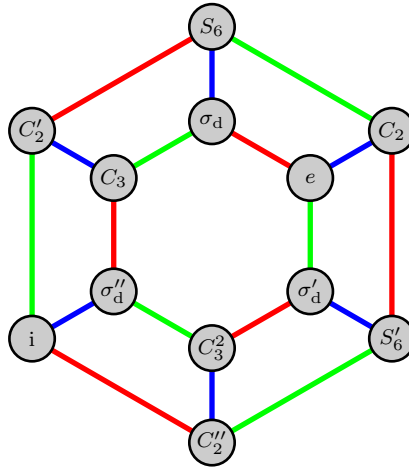


Figure 5: Cayley graph for the 3-protic acid dissociation. Red, green and blue edges represent the action of the generators σ_d , σ'_d , and C_2 , respectively.

In these compositions the product is taken from left to right. There are other compositions not shown. A global view of the group $\text{aut}(G_3)$ is given by the Cayley graph shown in figure 5. This graph shows two hexagonal cycles, both generated by σ_d and σ'_d , and connected by blue edges. The inner and outer hexagons are groups by themselves, both generated by σ_d and σ'_d . This is the condition of the dihedral group of order 6, D_3 . The change of generators from σ_d and σ'_d to σ_d and $C_3 = \sigma_d \sigma'_d$ gives the symmetric group S_3 , which is isomorphic to D_3 . The 12 graph automorphisms given by the permutations e and (78)–(89) are the

elements of the group $\text{aut}(G_3) = C_2 \times S_3$, which is isomorphic to the abstract dihedral group D_6 and the antiprismatic 3D point group D_{3d} (Schoenflies' notation).

The dissociation of the 4-protic acid is represented by a graph G_4 with $\text{aut}(G_4) = C_2 \times S_4$, a group of order 48. In general, an N -protic acid will have a graph G_N with graph automorphism group $\text{aut}(G_N) = C_2 \times S_N$ which has order $2N!$, and it is the direct product of the cyclic group C_2 and the symmetric group S_N .

Concluding remarks

The description of the micro-dissociation of an N -protic acid in terms of set theory is utilized to derive mathematical relations between equilibrium and micro-equilibrium dissociation constants. These mathematical relations are more convenient to use compared to the formulas based on indexation provided by Hill [51]. The advantages of our formalism are demonstrated by deriving equations that relate the equilibrium and micro-equilibrium constants of diprotic and triprotic acids.

Graph theory has been employed to represent and classify the micro-dissociation equilibrium of polyprotic acids as graphs, denoted as G_N , with the dissociation micro-states as vertices and the pairs of vertices connected by micro-dissociation constants as edges. Tautomerizations and acid-base reactions are treated as permutations on the vertex set of the polyprotic acid graph. It is shown that these permutations are graph automorphisms, and the composition of two of these permutations is also a graph automorphism. The set of automorphisms, endowed with composition, forms the automorphism group of the graph G_N . The generators of these groups were completely identified for monoprotic, diprotic and triprotic acids. In the case of monoprotic acids the graph automorphism group is given by the cyclic group C_2 . The analysis of the dissociation of a diprotic acid reveals the direct product $C_2 \times C_2$. Finally, the triprotic acid micro-dissociation of triprotic acids is represented by the direct product of the cyclic group C_2 and the symmetric group S_3 , denoted as $C_2 \times S_3$.

The Cayley graph for triprotic acid illustrates how the three generators are sufficient to classify the micro-dissociation of these acids. It is shown that for an N -protic acid the direct product $C_2 \times S_N$ is the graph automorphism group. The formalism and results presented in this paper enhance and broaden our understanding acid-base equilibrium.

Acknowledgments

This work has been partially funded by OMICAS Program: In-silico Multiscale Optimization of Sustainable Agricultural Crops (Infrastructure and validation in Rice and Sugar Cane) sponsored within the Scientific Colombia Ecosystem, made up by the World Bank, Ministry of Science, Technology, and Innovation (Minciencias), Icetex, Ministry of Education and Ministry of Industry and Tourism, Project ID: FP44842-217-2018. Partial funding was also provided by the internal research grants of Universidad Icesi.

The authors express their sincere gratitude to Professor Mathew Macauley of Clemson University for his invaluable insights and generous correspondence regarding group theory and graphical representation of groups.

Disclosure statement

No potential conflict of interest was reported by the authors.

References

- (1) Cayley, LVII. On the mathematical theory of isomers. *The London, Edinburgh, and Dublin Philosophical Magazine and Journal of Science* **1874**, *47*, 444–447.
- (2) Cayley, F. R. S. On the Analytical Forms called Trees, with Applications to the Theory of Chemical combinations. *Rept. Brit. Assoc. Adv. Sci.* **1875**, *45*, 257.
- (3) Brunel, G. Polymérisation du carbone. *Proc-verb. soc. Sci. Phys. Nat. Bordeaux* **1894**, 8–10.

- (4) Brunel, G. Sur la représentation graphique des isomères. *Proc-verb. soc. Sci. Phys. Nat. Bordeaux* **1898**, 108–110.
- (5) Rouvray, D. H. Isomer enumeration methods. *Chem. Soc. Rev.* **1974**, *3*, 355–372.
- (6) Rouvray, D. The pioneering contributions of Cayley and Sylvester to the mathematical description of chemical structure. *Journal of Molecular Structure: THEOCHEM* **1989**, *185*, 1–14.
- (7) Gutman, I. Georges Brunel - A Forgotten Pioneer of Chemical Graph Theory. *MATCH Commun. Math. Comput. Chem.* **2014**, *72*, 573–576.
- (8) Sylvester, J. J. On an Application of the New Atomic Theory to the Graphical Representation of the Invariants and Covariants of Binary Quantics, with Three Appendices. *American Journal of Mathematics* **1878**, *1*, 64–104.
- (9) Balaban, A. T., Ed. *Chemical Applications of Graph Theory*; Academic Press, 1976.
- (10) Trinajstić, N. *Chemical Graph theory*, 2nd ed.; CRC Press, 1992.
- (11) Bonchev, D., Rouvray, D. H., Eds. *Chemical group theory: introduction and fundamentals*; Mathematical Chemistry; Gordon and Breach Science Publishers, 1994; Vol. 3.
- (12) Bonchev, D., Rouvray, D. H., Eds. *Chemical group theory: techniques and applications*; Mathematical Chemistry; Gordon and Breach Science Publishers, 1994; Vol. 4.
- (13) Hashemi, A.; Bougueroua, S.; Gaigeot, M.-P.; Pidko, E. A. ReNeGate: A Reaction Network Graph-Theoretical Tool for Automated Mechanistic Studies in Computational Homogeneous Catalysis. *Journal of Chemical Theory and Computation* **2022**, *18*, 7470–7482, PMID: 36321652.
- (14) Droschinsky, A.; Humbeck, L.; Koch, O.; Kriege, N. M.; Mutzel, P.; Schäfer, T. In *Algorithms for Big Data: DFG Priority Program 1736*; Bast, H., Korzen, C., Meyer, U., Penschuck, M., Eds.; Springer Nature Switzerland: Cham, 2022; pp 76–96.
- (15) Branco, D.; Di Martino, B.; Cosconati, S.; Kranzlmüller, D.; D’Angelo, S. Towards a Parallel Graph Approach to Drug Discovery. *Advanced Information Networking and Applications*. Cham, 2023; pp 127–135.
- (16) Clarke, B. L. Stability analysis of a model reaction network using graph theory. *The Journal of Chemical Physics* **1974**, *60*, 1493–1501.

- (17) Clarke, B. L. *Advances in Chemical Physics*; John Wiley & Sons, Ltd, 1980; pp 1–215.
- (18) Temkin, O. N.; Zeigarnik, A. V.; Bonchev, D. G. Application of Graph Theory to Chemical Kinetics. Part 2. Topological Specificity of Single-Route Reaction Mechanisms. *Journal of Chemical Information and Computer Sciences* **1995**, *35*, 729–737.
- (19) Temkin, O. N.; Zeigarnik, A. V.; Bonchev, D. *Chemical Reaction Networks: A graph-theoretical approach*; CRC Press, Taylor & Francis Group, 1996.
- (20) Zeigarnik, A. V.; Temkin, O. N.; Bonchev, D. Application of Graph Theory to Chemical Kinetics. 3. Topological Specificity of Multiroute Reaction Mechanisms. *Journal of Chemical Information and Computer Sciences* **1996**, *36*, 973–981.
- (21) Feinberg, M. *Foundations of Chemical Reaction Network Theory*; Springer, 2019.
- (22) Futamata, N.; Yamamura, R.; Trinh Ha, D.; Takahashi, O. Fragmentation pathways of methylbenzoate cations following core excitation: Theoretical approach using graph theory. *Chemical Physics Letters* **2021**, *766*, 138316.
- (23) Rupp, M.; Körner, R.; Tetko, I. V. Estimation of Acid Dissociation Constants Using Graph Kernels. *Molecular Informatics* **2010**, *29*, 731–740.
- (24) Johnston, R. C.; Yao, K.; Kaplan, Z.; Chelliah, M.; Leswing, K.; Seekins, S.; Watts, S.; Calkins, D.; Chief Elk, J.; Jerome, S. V.; Repasky, M. P.; Shelley, J. C. Epik: pKa and Protonation State Prediction through Machine Learning. *Journal of Chemical Theory and Computation* **2023**, *19*, 2380–2388, PMID: 37023332.
- (25) Zhang, J. H.; Ricard, T. C.; Haycraft, C.; Iyengar, S. S. Weighted-Graph-Theoretic Methods for Many-Body Corrections within ONIOM: Smooth AIMD and the Role of High-Order Many-Body Terms. *Journal of Chemical Theory and Computation* **2021**, *17*, 2672–2690, PMID: 33891416.
- (26) Jacobs, D. J.; Rader, A.; Kuhn, L. A.; Thorpe, M. Protein flexibility predictions using graph theory. *Proteins: Structure, Function, and Bioinformatics* **2001**, *44*, 150–165.
- (27) Gligorijević, V.; Renfrew, P. D.; Kosciolk, T.; Leman, J.; Berenberg, D.; Vatanen, T.; Chandler, C.; Taylor, B. C.; Fisk, I. M.; Vlamakis, H.; Xavier, R. J.; Knight, R.; Cho, K.; Bonneau, R. Structure-based protein function prediction using graph convolutional networks. *Nat. Commun.* **2021**, *12*, 3168.

- (28) Siemers, M.; Lazaratos, M.; Karathanou, K.; Guerra, F.; Brown, L. S.; Bondar, A.-N. Bridge: A Graph-Based Algorithm to Analyze Dynamic H-Bond Networks in Membrane Proteins. *Journal of Chemical Theory and Computation* **2019**, *15*, 6781–6798, PMID: 31652399.
- (29) Godsil, C.; Royle, G. *Algebraic graph theory*; Springer, 2001.
- (30) Biggs, N. *Algebraic graph theory*, 2nd ed.; Cambridge University Press, 1993.
- (31) Razinger, M.; Balasubramanian, K.; Munk, M. E. Graph automorphism perception algorithms in computer-enhanced structure elucidation. *Journal of Chemical Information and Computer Sciences* **1993**, *33*, 197–201, PMID: 8314927.
- (32) Balasubramanian, K. Computational Techniques for the Automorphism Groups of Graphs. *Journal of Chemical Information and Computer Sciences* **1994**, *34*, 621–626.
- (33) Balasubramanian, K. Graph theoretical perception of molecular symmetry. *Chemical Physics Letters* **1995**, *232*, 415–423.
- (34) Randić, M. Aromaticity of Polycyclic Conjugated Hydrocarbons. *Chemical Reviews* **2003**, *103*, 3449–3606, PMID: 12964878.
- (35) Tratch, S.; Zefirov, N. Symmetry specified enumeration of substituted derivatives: an easy solution to the complex problem. *Russ. Chem. Bull.* **2008**, *57*, 235–252.
- (36) Petrucci, R.; Herring, F.; Madura, J.; Bissonnette, C. *Petrucci's General Chemistry: Modern Principles and Applications*, eBook; Pearson Education, 2023.
- (37) Atkins, P.; Jones, L. *Chemical Principles*; W. H. Freeman, 2008.
- (38) Harris, D.; Lucy, C. *Quantitative Chemical Analysis*, 10th ed.; W. H. Freeman, 2019.
- (39) Skoog, D. A.; West, D. M.; Holler, F. J.; Crouch, S. R. *Fundamentals of Analytical Chemistry*, 10th ed.; Cengage, 2021.
- (40) Denbigh, K. G. *The Principles of Chemical Equilibrium: With Applications in Chemistry and Chemical Engineering*, 4th ed.; Cambridge University Press, 1981.
- (41) Stumm, W.; Morgan, J. *Aquatic Chemistry: Chemical Equilibria and Rates in Natural Waters*; Environmental Science and Technology: A Wiley-Interscience Series of Texts and Monographs; Wiley, 2012.

- (42) Adams, E. Q. Relations Between the Constants of Dibasic Acids and of Amphoteric Electorolytes. *Journal of the American Chemical Society* **1916**, *38*, 1503–1510.
- (43) Mchedlov-Petrosyan, N. Polyprotic Acids in Solution: is the Inverse of the Constants of Stepwise Dissociation Possible? *Ukrainian Chemistry Journal* **2019**, *85*, 3–45.
- (44) Yatsimirskii, K. B.; Chekman, I. S.; Budarin, L. I.; Romanenko, É. D.; Frantsuzova, S. B. NMR Spectra and microequilibrium constants in izadrin (isadrine) and teranol solutions. *Theor. Exp. Chem.* **1978**, *13*, 262–267.
- (45) Noszál, B. Group constant: A measure of submolecular basicity. *The Journal of Physical Chemistry* **1986**, *90*, 4104–4110.
- (46) Hernández-Borrell, J.; Montero, M. T. Calculationg Microspecies Concentration of Zwitterion Ampho-
teric Compounds: Ciprofloxacin as Example. *Journal of Chemical Education* **1997**, *74*, 1311.
- (47) Mazák, K.; Noszál, B. Advances in microspeciation of drugs and biomolecules: Species-specific con-
centrations, acid-base properties and related parameters. *Journal of Pharmaceutical and Biomedical
Analysis* **2016**, *130*, 390–403, Review Issue 2016.
- (48) Scholz, F.; Kahlert, H. Acid–base equilibria of amino acids: microscopic and macroscopic acidity con-
stants. *ChemTexts* **2018**, *4*.
- (49) Pálla, T.; Fogarasi, E.; Noszál, B.; Tóth, G. Characterization of the Site-Specific Acid-Base Equilibria
of 3-Nitrotyrosine. *Chemistry & Biodiversity* **2019**, *16*, e1900358.
- (50) Li, G.; Wang, Y.; Sun, C.; Liu, F. Determination of the microscopic acid dissociation constant of
piperacillin and identification of dissociated molecular forms. *Frontiers in Chemistry* **2023**, *11*.
- (51) Hill, T. L. Microscopic Equilibria in Ampholytes. *Journal of the American Chemical Society* **1943**, *65*,
2119–2121.
- (52) Laufer, D. A.; Gelb, R. I.; Schwartz, L. M. Carbon-13 NMR determination of acid-base tautomerization
equilibriums. *The Journal of Organic Chemistry* **1984**, *49*, 691–696.